Establishment of X-ray computed tomography traceability for additively manufactured surface texture evaluation

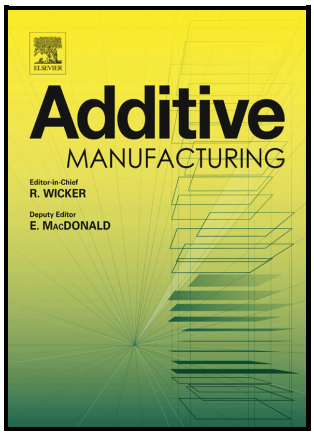

Wenjuan Sun, Claudiu Giusca, Shan Lou, Xiuyuan Yang, Xiao Chen, Tony Fry, Xiangqian Jiang, Alan Wilson, Stephen Brown, Hal Boulter

PII: S2214-8604(21)00705-3

DOI: https://doi.org/10.1016/j.addma.2021.102558

Reference: ADDMA102558

To appear in: *Additive Manufacturing*

Received date: 7 September 2021
Revised date: 7 December 2021
Accepted date: 10 December 2021

Please cite this article as: Wenjuan Sun, Claudiu Giusca, Shan Lou, Xiuyuan Yang, Xiao Chen, Tony Fry, Xiangqian Jiang, Alan Wilson, Stephen Brown and Hal Boulter, Establishment of X-ray computed tomography traceability for additively manufactured surface texture evaluation, *Additive Manufacturing,* (2021) doi:https://doi.org/10.1016/j.addma.2021.102558

Additive Manufacturing, Available online 14 December 2021, Article number 102558
DOI:10.1016/j.addma.2021.102558

Establishment of X-ray computed tomography traceability for additively manufactured surface texture evaluation

Wenjuan Sun[1], Claudiu Giusca[2], Shan Lou[3], Xiuyuan Yang[1,2,] Xiao Chen[1,3], Tony Fry[1], Xiangqian Jiang[3], Alan Wilson[1], Stephen Brown[1], Hal Boulter[1]

[1]*Engineering Department, National Physical Laboratory, Hampton Road, Teddington, TW11 0LW, United Kingdom*

[2]*Surface Engineering and Precision Institute, Cranfield University, Cranfield, Bedfordshire MK430AL, UK*

[3] *EPSRC Future Metrology Hub, University of Huddersfield, Queensgate, Huddersfield, HD1 3DH, United Kingdom*

Abstract

Metal additively-manufactured (AM) parts are increasingly used as safety-critical components in industry. Surface textures of metal AM parts are different to conventionally machined surfaces and can directly influence the functional performance of the parts. However, it is difficult or impossible to access and measure non-line-of-sight AM surfaces by conventional measurement techniques. X-ray computed tomography (XCT) is a promising technique that can measure non-line-of-sight surfaces non-destructively. However, the metrology framework for XCT to evaluate surface texture of AM parts is yet to be fully established, and there is a lack of development in surface texture reference standards that fit the purpose.

In this paper, we have established a route to calibrate XCT for AM surface texture evaluation using a prototype three-dimensional roughness standard (3DRS) developed by the National Physical Laboratory that has a range of AM surface texture features and was designed for compatibility between 2D (profile), 2½D (areal), and tomography measuring instruments. A measurement protocol has been established between XCT and the contact stylus system, and uncertainty evaluation of 3DRS surface texture was established.

Keywords:

Additive manufacturing, surface texture, reference standard, X-ray computed tomography

1 Introduction

The ability of additive manufacturing technologies to build complex non-line-of-sight features offers vast design and manufacturing freedom yet challenges the traditional geometrical product specification (GPS) norms designed around conventional machining quality control requirements, consequently hindering its seamless integration in the stringent advanced manufacturing environment. From a GPS perspective, surface texture or roughness measurements have been long used in production to check the quality of manufactured products given the roughness' strong dependence on the process parameters and its strong relationship with the components' functionality, such as heat transfer [1] or fatigue life [2] in AM cases.

During the build process of AM surfaces, especially for the powder bed fusion-based technologies, the powder particle size, the layer thickness, beam power and incident angle, as well as the build orientation, are the key factors influencing the surface texture [3-5]. Surface texture of AM surfaces, ranges from tens to several hundred micrometres [6-9]. AM surface texture evaluation has been previously reviewed in the literature [10]. From comparing different measuring methods [11] to understand the relationship between the surface texture parameters and additive manufacturing process parameters [12-15] and proposing feature-based characterisation [16], the published research pointed out the problems incurred in surface texture measurements and analysis technology and the multiscale nature of AM surfaces and the relationship with the functionality of the components [17]. Despite the complexity of AM surfaces, industry is in need of simple characterisation tools akin to traditional profile evaluation that allow evaluating the process parameters effect on the quality of the manufactured components. It is worth pausing here to distinguish between the surface texture measurements used in research to tailor specific surface functionality and their application in the production control metrics. The first application relies on more exotic parameters that need areal characterisation (2½D) as discussed above, whereas the second application only requires a simple 2D parameter. To this end, some researchers discuss the effect of the periodic feature on the AM surface's waviness components [18], also classified as the stair effect [19], in contrast to other peers that contextualise it as surface roughness [20]. AM surface texture evaluation is still under development, with no standard clearly defining the waviness and roughness measurement bandwidths of AM surfaces. The obvious solution for AM surface texture measurements is to establish their traceability to the unit of length (the metre) via the surface texture measurement traceability infrastructure [21].

More recently, due to the concealed nature of the surfaces (non-line-of-sight features), the use of X-ray computed tomography (XCT) has been proposed as a practical surface texture measuring tool [22, 23]. There are a considerable number of publications concerning uncertainty evaluation, and implicitly measurement traceability, of a restricted number of simple geometrical characteristics (size, distance, and form [24]) using XCT [25-27]. Measurement of AM surfaces texture using XCT is a growing subject in recent years, but there is an apparent lack of confidence in such XCT measurements [22].

Preliminary studies demonstrated that XCT technique is able to quantify both external and internal surface texture of AM components, and the results have been compared to optical instruments, such as focus variation and confocal microscope instruments [22, 28, 29]. To circumvent the lack of traceability of the optical instruments, some researchers have used 2D optical techniques to measure the cross-sectional profile of the surfaces obtained following cutting and polishing the samples [29]. However, contacting measurement techniques, including tactile coordinate measuring systems (CMS) and profile contact stylus (CS) instruments, are generally accepted as reference instruments to provide traceable measurements of form and surface texture respectively [30, 31]. The comparison between XCT and CS have been conducted in [29, 32], with the focus on the primary texture profiles. The measurement uncertainty evaluation of surface texture using XCT has been explored based on the comparator method - a technique for determining the uncertainty of measurement use of calibrated workpieces or measurement standards [29], but the uncertainty associated with *Pa* measurement results was found to be as high of 23% of the *Pa* value [29].

When evaluating measurement uncertainty using calibrated reference standards, the surface texture of the standard should reproduce the range and morphology of the typical AM surfaces [33]. In recent years, AM technologies progressed with better manufacturing optimisation and post-processing [34, 35]. Surfaces of finished AM parts can be significantly smoothed in contrast to as-built AM surfaces. For production purposes, as-built AM surfaces can be easily evaluated using visual inspection. However, post-processing often removes the re-entrant features and reduces the roughness to micrometre level [36-38]. The AM industry requires reference standards that can be used as surface texture comparison specimens or roughness comparators [10, 39, 40], similar to those used to evaluate the surface textures of components manufactured using traditional subtractive machining techniques, such as milling, turning, grinding, polishing [41]. In this context, the design of AM surface texture reference standard should consider a range of surface roughness levels. The design should

also allow the comparison between XCT and reference measurement techniques. Often for traditional manufacturing processes, handheld roughness measuring instruments are used in conjunction with roughness comparators for routine assessment of conventional machining surfaces. There are reference samples developed in recent years, but most of them focus on a single aspect of the requirement [22, 42]. Measurement capability, such as measurement range and sampling distance, have to be considered together with the design of the standard, such as surface orientation, level of surface roughness and additional features for data registration.

The other challenge is associated with the measurement bandwidth limitation of different measurement techniques. The distinct volumetric measurement ability of XCT and the size of the voxel makes it difficult to match the bandwidth of operation of the 2D or 2½D traceable surface texture instruments [11, 43]. The typical voxel size of XCT is in the range of micrometres to a couple of hundreds of micrometres compared to the nanometres order vertical resolution and sub-micrometre lateral resolution of traditional roughness measurement instruments, limiting XCT's ability to measure high spatial frequencies [44]. High-resolution XCT instruments come at the expense of texture evaluation length, hence, inhibiting the statistical relevance of the roughness parameters for most AM applications. Besides XCT's bandwidth mismatch conundrum, AM surfaces challenge the underlying definitions and assumptions of traditional surface texture evaluation [23, 29], from filtration cut-offs to the contribution of the re-entrant features to the texture parameters, adding additional layers of complexity in the development of measurement traceability and, probably most importantly, preventing AM technologies to establish their own quality production standards.

Recent publications document the efforts of various researchers with deep roots in precision engineering seeking to develop calibration solutions to solve roughness traceability issues. Most of the methods use the Metrological Characteristics (MC) framework of surface topography instruments [45, 46], which allows estimation of the uncertainty associated with texture measurements as a function of limited input parameters such as amplification and linearity of the scales and noise. The uncertainty contribution of each MC is estimated using specific measurement methods and reference samples to reduce the sensitivity of the result to the other MCs in the set. The MC based measurement model used to evaluate the uncertainty associated with the traditional surface texture instruments is well documented [46], and currently, standardisation work is nearly completed. However, the MC approach for XCT

traceability is filled with perils mostly driven by the complex contribution of influence factors of the industrial XCT such as magnification (which determine the voxel size of XCT measurements), X-ray spectrum, beam hardening artefacts and scattering artefacts etc. To overcome the lack of a comprehensive MC calibration of XCT, the recent trend to establish traceability and uncertainty evaluation of XCT follows the guidance in ISO 15530-3 for CMSs. ISO 15530-3, Technique for determining the uncertainty of measurement - Use of calibrated workpieces or measurement standards [47] framework introduces the procedure to establish traceable measurements and measurement uncertainty and does not require the evaluation of uncertainty due to individual influence factors. The method relies on calibrated reference standards or workpieces. However, as previously discussed, there is limited work focusing on surface texture evaluation implementing this approach. The equivalent surface texture implantation of the ISO 15530-3 relies on Type D roughness measurement standard [48] and the standard rules of roughness assessment [49] and allow to evaluate/calibrate the overall performance of the surface texture measuring instruments, with the caveat that traditional profile standardisation is not immediately applicable for AM and XCT case and only can be used as guidance.

In this paper, we have investigated the use of roughness comparators to calibrate the XCT measurement of powder bed fusion technologies - the most common additive manufacturing technologies producing metallic components. The scope is limited to 2D traceability or specifically to the arithmetic mean deviation of the assessed profile, commonly known as *Ra* [50], one of the basic and most used parameters used in industry, hence our chosen example. A discussion on the 2½D case will be provided in a subsequent paper, as it requires additional considerations [10]. The typical surface roughness level of *Ra* is between 10 µm to 40 µm [35]. The traceability and uncertainty evaluation of surface texture is based on the methods defined in [49] and GUM [51], which mirror the ISO 15530-3. We also constraint some measurement settings to mimic the measurement conditions likely encountered at shop floor. This is different to the strategy used in literatures to study the uncertainty contributions of MC, where a worst scenario is often considered.

2 Experimental approach

2.1 Reference sample

The focus of the research is to calibrate XCT instrument(s) for surface texture measurements. For this, we have used the prototype of the 3D roughness standard (3DRS) designed by the National Physical Laboratory (NPL), shown in Figure 1. The 3DRS was manufactured by electron beam melting, which is a popular additive manufacturing technology used in industry. The material used, Ti64 alloy, is also a typical material for many industrial applications. The design of the sample accommodates three distinct sets of features: spheres, one-sided steps (ST), and roughness features. The sample has four faces (A, B, C, and D). Five high precision zirconium spheres with 2 mm diameters and low form error are mounted on the 3DRS: two on face A and three on the other three faces (see Figure 1). The holes were milled at NPL at specific positions to a predefined depth, allowing approximately 50% of the spheres to protrude from the AM surface. The protruded spheres could then allow tactile measurements to be conducted to define the sphere position. The spheres were fixed in position using adhesive placed at the base of the milled recess. Different roughness features are present on the four faces. Face A is the as-built surface. The other three faces (B, C, and D) were then bead blasted to create different levels of roughness. Electrical discharge machining (EDM) has been used to produce the terraces of the steps resulting in micrometre level surface roughness.

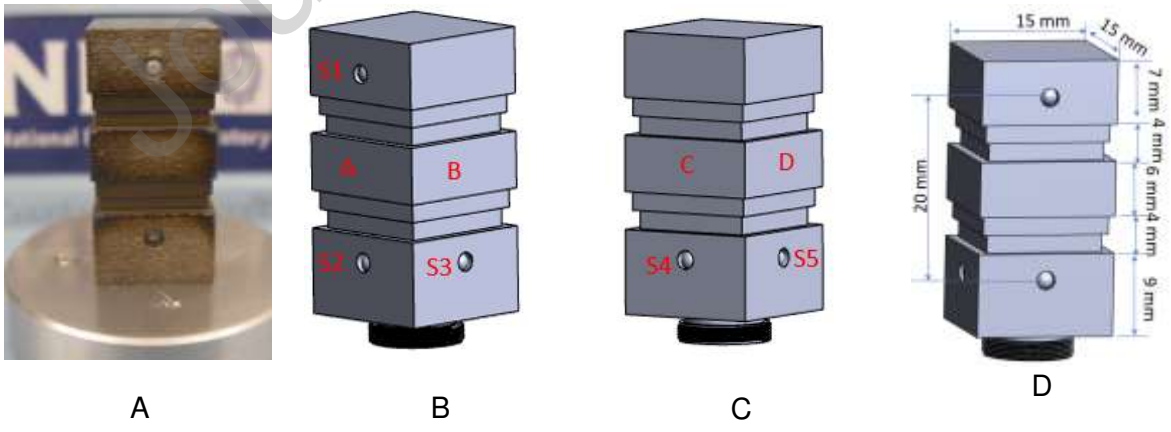

Figure 1 Photograph of the prototype of NPL's 3DRS. A. Photo of the sample. B and C. Schematic drawing. D. Nominal size of the part.

The reference standard was designed to address the calibration of the overall surface texture measurement. In XCT, voxel size represents the scale of measurement. Although the main objective of the research was to investigate the traceability of XCT for surface texture measurements, voxel size calibration has been considered as it is an essential task that deals with the use of XCT at different magnifications.

2.2 Instruments and measurements

Measurements were taken using a Nikon XT H 225M, a metrological industrial XCT system. The instrument is a cone-beam XCT system with a reflection tungsten target and a flat panel detector. Both the X-ray tube and the detector were stationary. The measurements of the prototype 3DRS were conducted using X-ray generator settings of 180 kV, 120 µA, with a 0.5 mm copper filter, with no additional calibration prior to the measurements. The flat-panel detector has 2000 × 2000 pixels with a pixel size of 200 µm × 200 µm. The measurements were circular scans with a magnification of 10 and reconstructed data has a voxel size of 20 µm × 20 µm× 20 µm. The 3DRS sample was positioned upright on the rotation stage in the XCT system. Between measurements, the sample was taken entirely off the rotational stage and then put back so that position and orientation of the sample were different in each measurement.

Two contact types of instruments were used to provide traceable measurements:

- A CMS, Zeiss F25 system, with a probe diameter of 0.125 mm and measurement uncertainty of 50 nm (k = 1). This instrument was used to measure the spheres on the 3DRS. It should be noted that the CMS calibration route is used here only to contextualise the voxel size contribution to the surface texture measurements.
- A CS [31], Taylor Hobson's Talysurf PGI 1000, was used to measure the surface texture on the ST's plateaus and the roughness features of the faces A, B, C, and D of the 3DRS. The stylus was fitted with a diamond conisphere with a 60º angle and a 2 µm radius tip [48]. The CS has a height measurement uncertainty of 43.7 nm (k = 1). The sampling distance of measurements conducted was 0.125 µm.

All measurements have been repeated three times to evaluate the reproducibility and repeatability of results. Before each measurement, the sample has been repositioned. All

measurements were conducted after X-ray has been switched on for 10 minutes to avoid drifting effects [52].

2.3 Voxel size calibration

The voxel size of reconstructed volume by default is defined as $\frac{SDD}{SOD} * detector\ pixel\ size$, where SDD stands for the source to detector distance, SOD is the source to object distance and $\frac{SDD}{SOD}$ is the magnification. SDD is nominally considered fixed for industrial cone-beam XCT systems, whereas SOD varies to accommodate the sample size and measurement resolution, leading to different magnifications. Positioning variation of the focal spot, thermal expansion of the instruments' mechanical components and positioning accuracy of the rotary stage can all affect the SDD and SOD values, but system warm-up can eliminate the issue [52].

Voxel size calibration provides the means to establish the scale correction factor (or the effective voxel size) and the traceability to the standard unit of length of the subsequent measurements. However, previous work shows that the XCT scale calibration plays a small role in the subsequent surface texture measurements [22]. The most common voxel size calibration technique relies on the centre-to-centre distance measurement between two or more reference spheres. The reference sphere measurement carries the advantage of a unidirectional measurement and eliminates beam hardening and scattering effects on the measurement accuracy.

In this study, the spheres on the face A, S1 and S2 as indicated in Figure 2, were measured using the contact CMS (see section 2.2) and used for voxel size calibration of the XCT instrument. In total, 102 data points were measured across the hemisphere surface protrude, and the data was fitted using the least-square sphere fitting algorithm. Corresponding analyses of XCT data used VGSTUDIO MAX 3.4.3 (VG) software with default settings in the sphere measurement section, where data across the sphere were selected and the least-square fitting algorithm was used.

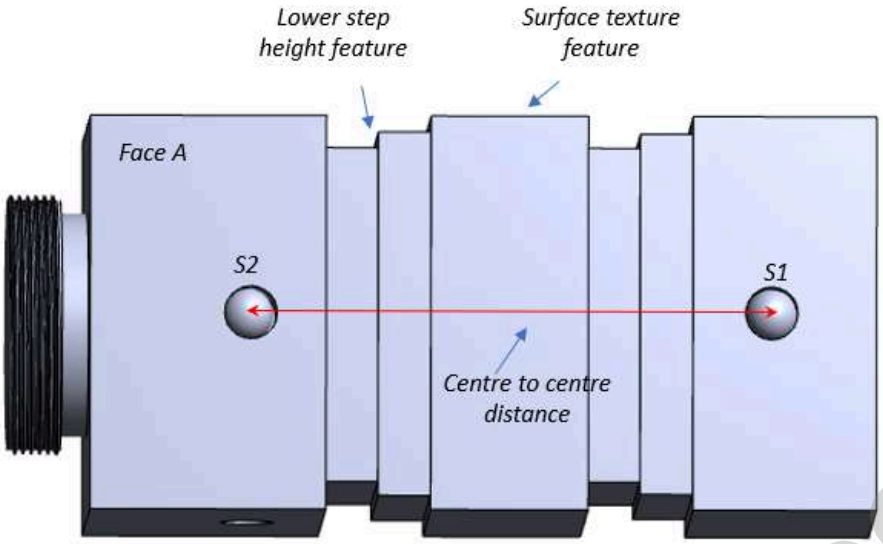

Figure 2 Features of 3DRS reference standard.

2.4 Surface roughness measurements

The surface texture features on the four faces (A, B, C, and D) of the 3DRS cover typical *Ra* values in the (10 to 30) µm interval. The ST was used to provide complementary surface roughness in the micrometre range, extending the lower end of the roughness calibration range.

The *Ra* was evaluated on profiles measured with CS across the axis of the 3DRS, as illustrated in Figure 3. The centres of spheres were used as datums for positioning reference for CS measurements. Six profiles were measured on each of the A, B, C, and D surfaces and four on the ST surface. The position and spacing between each profile are given in Figure 3. The extracted profiles were approximately 14 mm in length, apart from the four profiles measured on the step height region, which were slightly less due to materials removed by EDM machining.

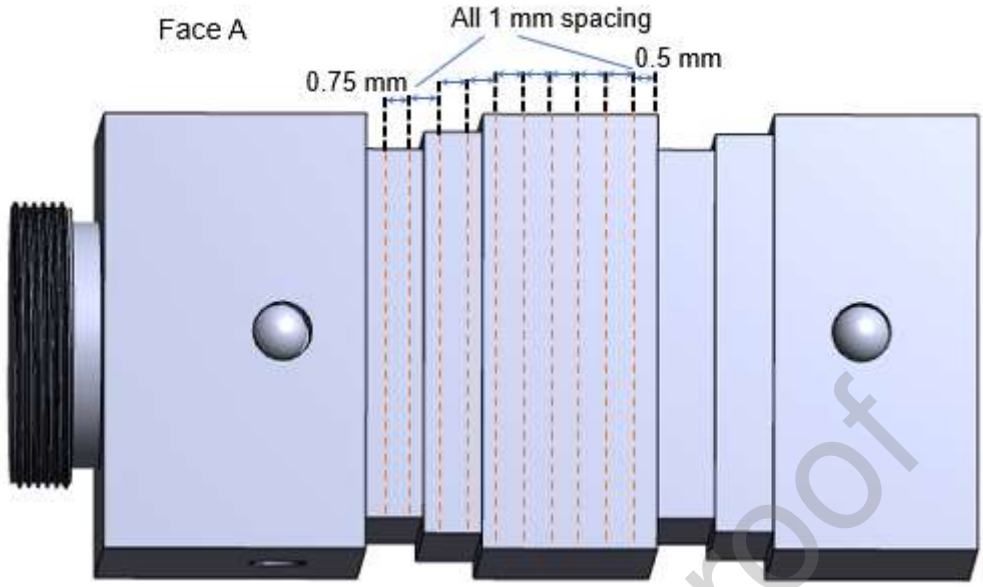

Figure 3 Measurement locations of the surface texture features.

The general guidance of surface profile measurement can be found in the literature [53]. Prior to *Ra* calculation, the profiles have been levelled using a least-square line fit, followed by a λs and λc filter to remove form, waviness and instrument noise [50]. The contact instrument CS measured profiles across the surface and the measurements were conducted with a small sampling interval 0.25 µm. The profiles have then been down-sampled to a 20 µm sampling distance to match the XCT's voxel size. Further details about the instrument bandwidth matching are provided in the discussion section. The roughness was analysed using Mountains® software version 8.2 from Digital Surf.

2.5 XCT data process

The XCT data was reconstructed using Nikon's CT Pro 3D software Version XT 5.4. A cross-section gray value image of the reconstructed volume data is shown in Figure 4. The reconstructed volumetric data was then processed using VG. The surface was determined using the Iterative Surface Determination function in the Advanced Mode in the Surface Determination module., where the algorithm for the surface edge with the consideration of local gray value gradient.

To determine the position of spheres, the surface data were selected with the default setting and the size was estimated using the least square method in VG software. The spheres of the 3DRS were primarily used to register the XCT measurement data as follows: centres of spheres S2, S3 and S4 were used to generate a plane, then centres of S2 and S4 provided a

line (line 1), and finally the projection of the centre of S3 to line 1 was used to establish the origin of the coordinate system.

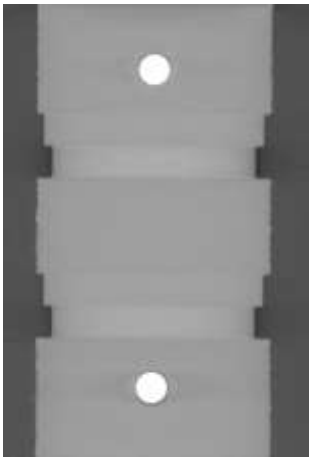

Figure 4 Cross-section image from volumetric data to show good contrast between the materials and the background.

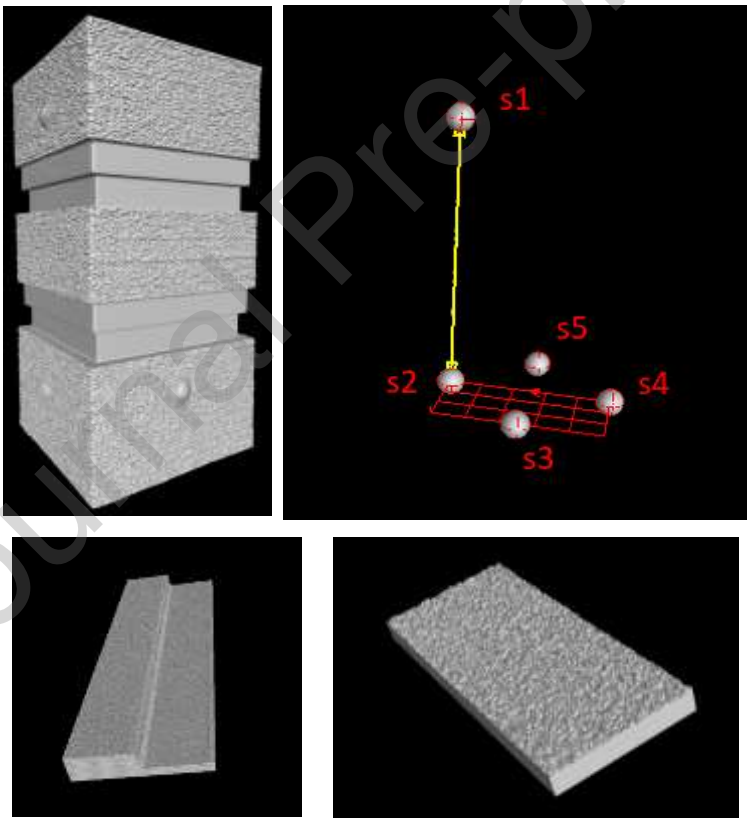

Figure 5 XCT measurement result of the 3DRS. Top left. Overall 3DRS sample. Top right. Sphere features. Bottom left. Bottom ST. Bottom right. Surface texture feature.

After the data registered, several steps were involved in the analysis workflow of the XCT measurements of ST and surface texture. First, the region of interest (ROI) that contained the feature to be evaluated was defined, features (sphere surfaces, the lower step height of face A and a surface texture) are shown in Figure 5. The surface within the ROI was then extracted

using the Ray-based method in the Convert to Mesh section in VG. The algorithm calculates the intersection of the surface with a regular, three-dimensional grid and a point is determined whenever the grid intersect the surface. In the process, a small tolerance (0.1 µm) was considered with no data simplification. The data was then converted into a uniform grid of points in MATLAB using linear interpolation. Once the surface data was extrapolated, corresponding analysis of spheres and surface texture evaluation was then conducted following the procedures given in sections 2.3 and 2.4.

3 Results and discussions

3.1 Voxel calibration – precision spheres

The measurement results of the centre-to-centre sphere distance are shown in Table 1.

Table 1 Length measurements results of centre-to-centre distance (1, 2, 3), means ($\bar{l}$) and standard deviation of the mean ($\sigma_{\bar{l}}$).

Id.	XCT	CMS
	/mm	
1	19.914 39	19.896 91
2	19.915 15	19.896 89
3	19.914 97	19.896 82
$\bar{l}$	19.914 84	19.896 87
$\sigma_{\bar{l}}$	0.000 23	0.000 027

From Table 1, the centre-to-centre measurements provide a correction factor for voxel size of 1.000903 with an associated combined standard measurement uncertainty [51] of 0.000021 (k = 1).

3.2 Roughness measurement bandwidth

Surface profile roughness measurements follow the guidance in [49]. Existing literature depicts the bandwidth matching challenges that occur during roughness evaluation of AM samples using different measuring instruments [54]. However, there are only two key parameters that define the roughness measurement bandwidth, λs and λc filters' cut-offs. λs filter removes the high spatial frequency components, and λc filter removes the waviness, which subsequently infers the roughness measurement conditions. More important here to stress is that roughness/surface texture measurements will have different results if they are performed at different bandwidths.

3.2.1 λ_S filter cut-off

λ_S filter defines the intersection between the roughness and the even shorter wave components [50]. For *Ra* larger than 10 µm, the λ_S cut-off value should be set at 8 µm. However, the voxel size of 20 µm of the XCT limits λ_S cut-off to roughly 80 µm. At a closer analysis of the CS results shown in Figure 6, it can be observed that the difference between 8 µm and 80 µm cut-offs bears no impact on the roughness profiles. The power spectrum analyses also show little difference by applying a different λ_S of 8 µm and 80 µm, which is in agreement with previous findings [44] and confirms that the dominant surface texture components have a spatial wavelength larger than 80 µm.

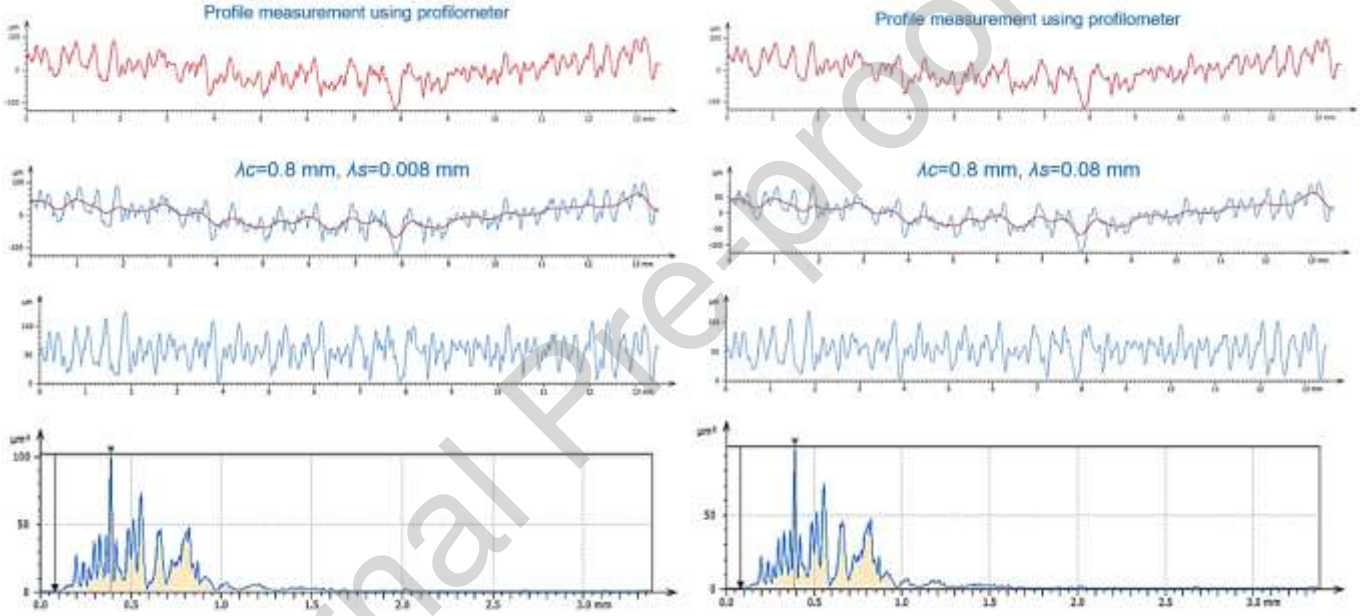

Figure 6 Comparison of data after application of different λs filters (the data is taken from CS measurements across the 3DRS reference standard). Top row: raw profile (blue) and data filtered with λ_S (red). Second row: data after filtered with λ_S (blue) and data further filtered with λ_c (red). Third row: remaining data after filtered with λ_S and λ_c. Bottom row: power spectrum analyses of the remaining data.

3.2.2 λ_C filter cut-off

λ_C defines the intersection between the roughness and waviness components, and its cut-off value is dependent on the value of *Ra*, which is mostly influenced by the relative height of the larger topographical features present on an AM surface. ISO 4288 recommends an 8 mm cut-off value for the *Ra* values reproduced by 3DRS, except for step height roughness, which requires a 0.8 mm cut-off [49]. However, the 8 mm cut-off requires an evaluation length of 40 mm, five times larger than the λ_C cut-off, and a total length of 48 mm to deal with the end effects of the filters. This length exceeds the length of the surface textures of the 3DRS. Practically, a sample with a greater length can be manufactured. However, when using XCT,

a longer sample cannot be fitted within the measurement volume with a cone-beam circular scan configuration while maintaining the same magnification. It is also costly to measure such long surfaces using optical scanning types of instruments.

As the most important surface texture features of the powder bed fusion manufactured surfaces are related to particle sizes and layer thickness, with the feature size at the tens or hundreds micrometre levels, two λ_C cut off-values, 2.5 mm and 0.8 mm, have been investigated. The 2.5 mm λ_C cut-off requires an evaluation length of 12.5 mm and 0.8 mm λ_C cut-off requires an evaluation length of 4 mm [49]. The effect of the two cut-off values was investigated on the CS measurement results and are presented in Figure 7. It can be seen that a 2.5 mm cut-off removes form errors and has a limited effect on the amplitude of the main surface texture features, which are limited to 1.7 mm spatial wavelength, whereas a 0.8 mm cut-off reduces the amplitude of some of the main roughness features. Similarly, the impact of λ_C cut-off on XCT measurement results are illustrated in Figure 8. The λs effect is neglectable due to the voxel size of XCT measurements. However, the λ_C cut-off of 0.8 mm appears to filter some of the effects of the XCT errors that influence the overall shape of the measured component.

Table 2 shows the result of surface texture evaluations made by the CS and XCT system, using λs of 80 µm. The evaluation has considered λc of both 2.5 mm and 0.8 mm. The data of the CS has also been down-sampled to a spacing of 20 µm, which matches the spacing of the XCT measurements.

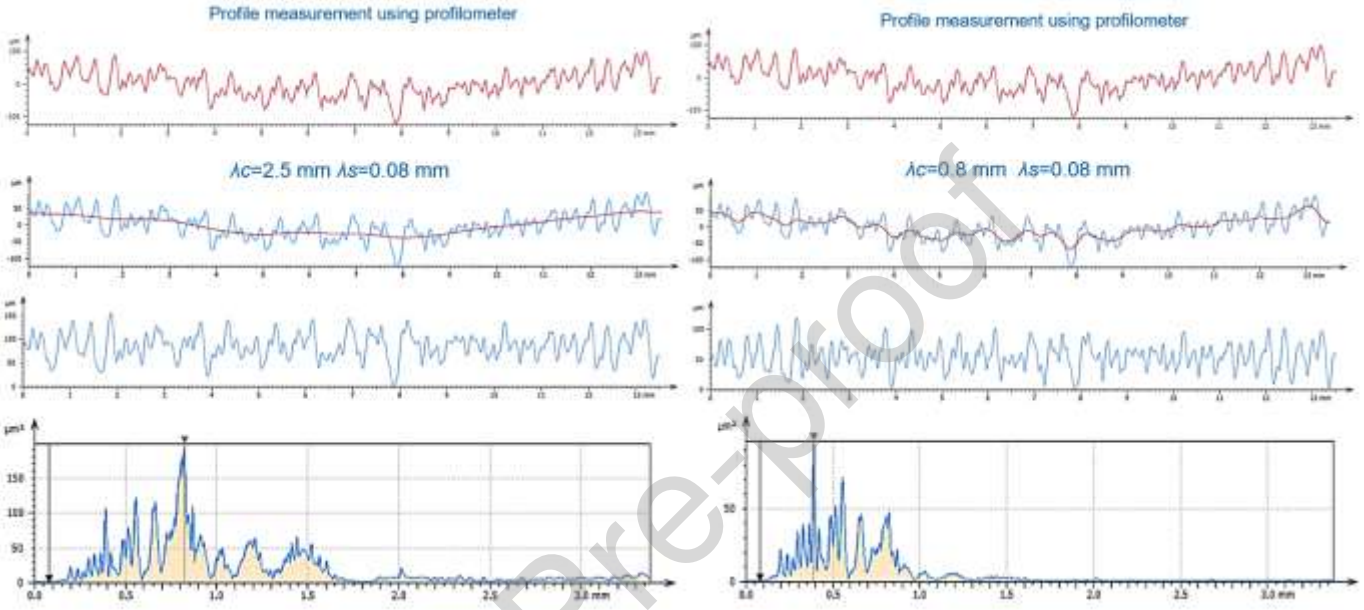

Figure 7 Comparison of data with application of different λc filters (the data is taken from CS measurements across the 3DRS reference standard). Top row: raw profile (blue) and data filtered with λ_S (red). Second row: data after filtered with λ_S (blue) and data further filtered with λ_c (red). Third row: remaining data after filtered with λ_S and λ_c. Bottom row: power spectrum analyses of the remaining data.

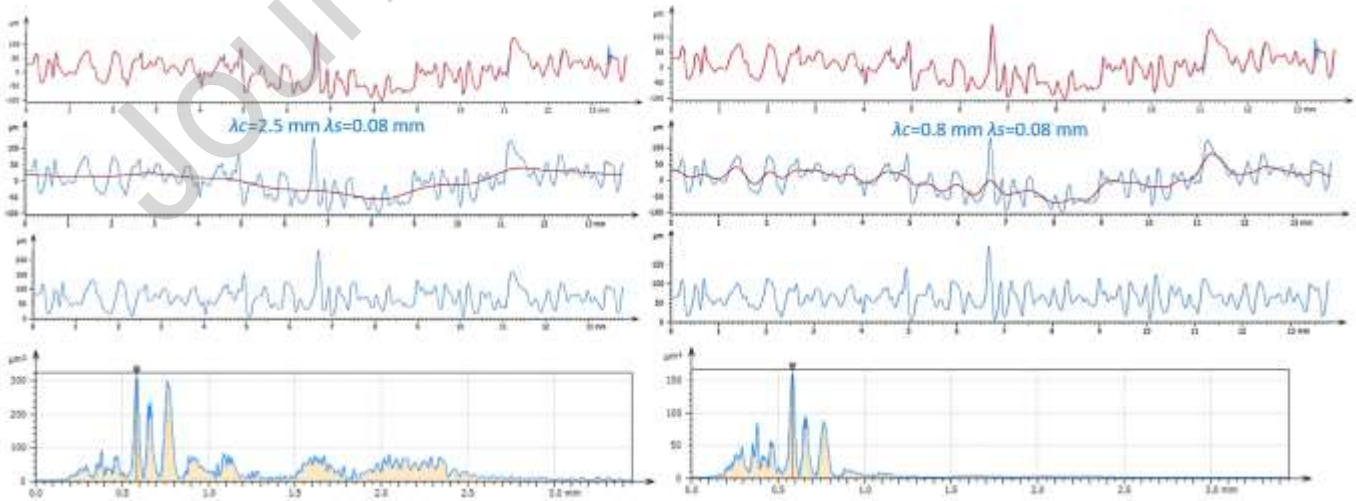

Figure 8 Comparison of data with application of different λc filters (the data is taken from XCT measurements across the 3DRS reference standard). Top row: raw profile (blue) and data filtered with λ_S (red). Second row: data after filtered with λ_S (blue) and data further filtered with λ_c (red). Third row: remaining data after filtered with λ_S and λ_c. Bottom row: power spectrum analyses of the remaining data.

Table 2 Surface texture evaluation using a λs=80 µm cut-off, where $\overline{Ra}$ is the mean of the arithmetic mean deviation of the six assessed profiles on the faces A to D and of the four profiles on the ST, and $\sigma_{\overline{Ra}}$ is their corresponding standard deviation of the mean.

λc/ mm	Measurement Id	Face A	Face B	Face C	Face D	SH surface
		$\overline{Ra} \pm \sigma_{\overline{Ra}}$ /µm				
0.8	CS					
	1	17.00 ± 0.56	14.79 ± 0.55	11.04 ± 0.57	13.33 ± 0.50	1.44 ± 0.05
	2	17.01 ± 0.56	14.73 ± 0.59	11.04 ± 0.58	13.33 ± 0.50	1.43 ± 0.06
	3	17.01 ± 0.56	14.70 ± 0.56	11.05± 0.56	13.30 ± 0.50	1.41 ± 0.05
	XCT					
	1	19.26 ± 0.63	15.70 ± 0.59	11.22 ± 0.59	15.55 ± 1.03	0.87 ± 0.03
	2	19.30 ± 0.70	15.53 ± 0.63	11.16 ± 0.53	15.66 ± 1.00	0.84 ± 0.01
	3	19.49 ± 0.51	15.11 ± 0.96	11.32 ± 0.66	15.82 ± 1.04	0.8 ± 0.01
2.5	CS					
	1	23.36 ± 1.08	20.29 ± 0.95	15.96 ± 0.95	19.99 ± 0.58	1.55 ± 0.04
	2	23.46 ± 1.23	20.40 ± 0.98	16.00 ± 0.93	19.99 ± 0.62	1.54 ± 0.05
	3	23.37 ± 1.15	20.30 ± 1.00	15.99 ± 0.94	19.91 ± 0.58	1.56 ± 0.05
	XCT					
	1	26.40 ± 0.49	21.34 ± 0.81	16.24 ± 0.85	22.63 ± 1.92	1.00 ± 0.05
	2	26.19 ± 0.56	21.22 ± 0.64	16.00 ± 0.83	22.41 ± 1.91	0.95 ± 0.02
	3	26.52 ± 0.40	21.74 ± 1.31	16.00 ± 0.90	22.47 ± 1.91	0.94 ± 0.03

3.3 Error analysis

Figure 9 illustrates a comparison between XCT and CS measurement results across face B. It is not always possible to compare the measurement of the same surface profile when using two instruments. Even with a carefully designed datum and sampling strategy, and when the profiles are sampled in a close enough region, the residual errors between the two profiles are as large as 50 % of profile's peak to valley ranges despite the relatively small difference in *Ra* values, which is in excess of 6 %. However, the relative difference between the XCT and CS *Ra* values is not maintained across different roughness levels reproduced by the sample, indicating a non-linear relationship between the amplitude parameters values and their corresponding bias, which cannot be attributed to the linear scale dependent error, but rather to the instruments' transfer function.

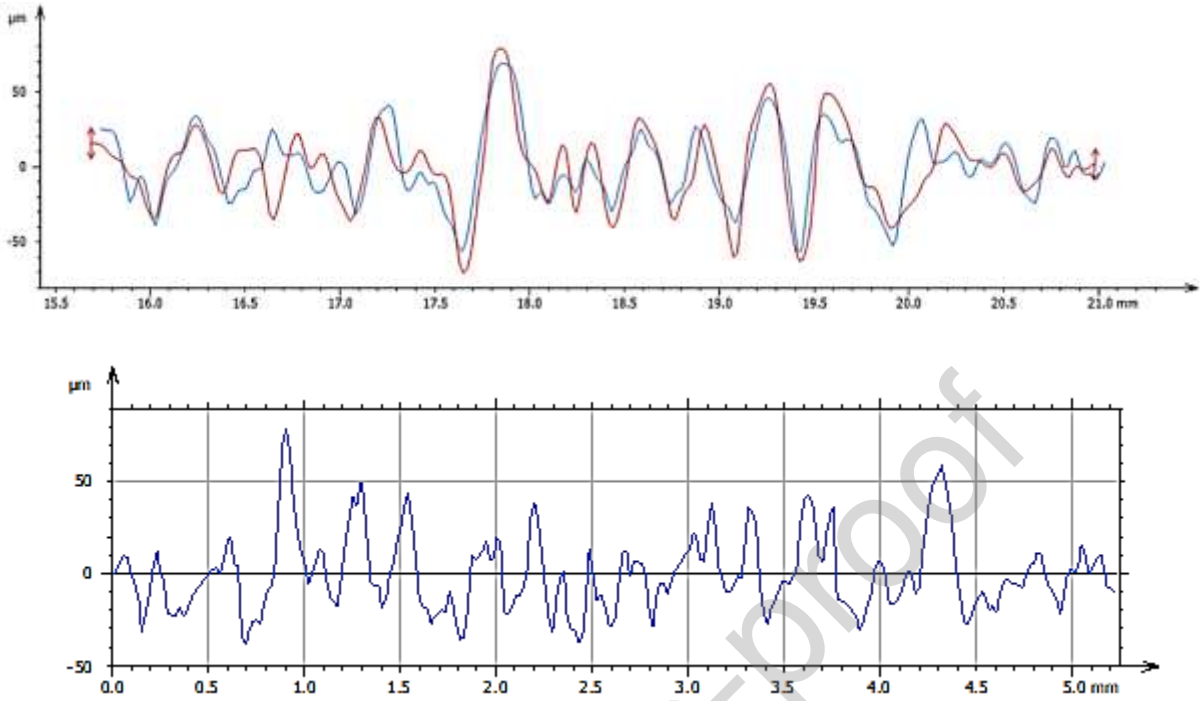

Figure 9 Comparison of surface texture measurements using XCT and tactile probing on face B. Top - red is XCT, blue is CS. Both data were levelled and obtained using λc=0.8 mm and λs=0.08 mm filters. The CS data was down-sampled to 20 µm spacing. Bottom – the difference between CS and XCT results.

In the case of the CS, stylus flanking is one of the potential sources of errors. An example of stylus flanking is shown on a profile extracted across the ST plateaus is shown in Figure 10. However, when stylus morphological effect is simulated on the XCT measured profiles, the resulting *Ra* values account for less than 10 % of the error between the XCT and CS results. An example of impact of the stylus measurements on surface texture is shown in Figure 11.
As the roughness is reduced to the level of the EDM surface finish present on the ST surface, the XCT severely attenuates the height of the profiles to almost 50 %, as shown in Figure 10 left inset. Here the voxel size suppresses the effect of small spatial wavelengths present on the surface.

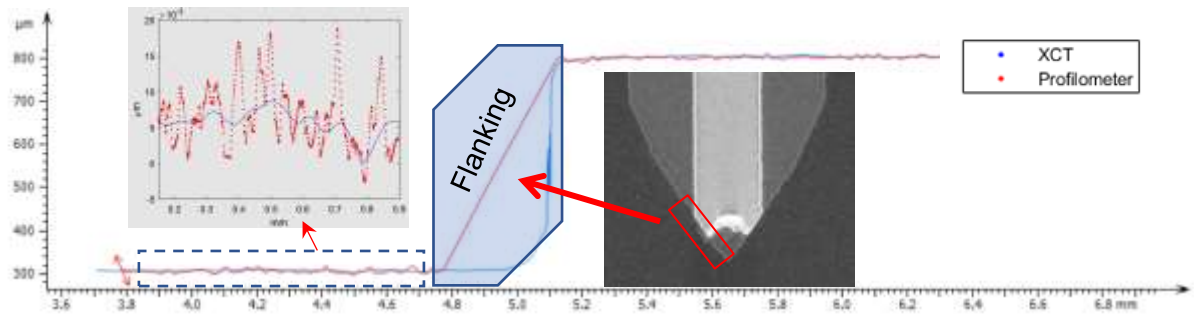

Figure 10 XCT and profilometer measurement results on the step height feature. Left inset is a section of the profile measured on the lower plateau of the ST. Right inset is an XCT image of the stylus tip.

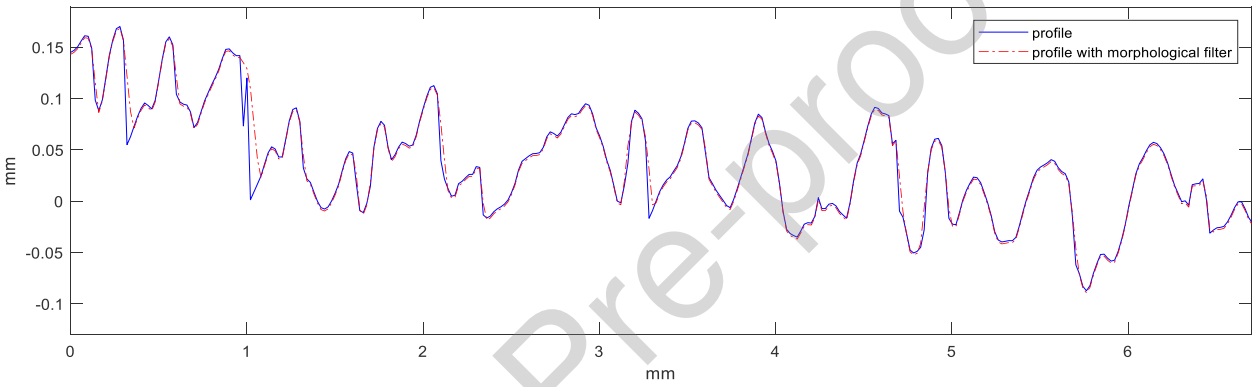

Figure 11 Illustration of profile measurement and the effect of impact of stylus tip.

The value held by the voxel represents an average of a surface area and is likely to be strongly correlated with the adjacent voxels, whereas to a first approximation, CS will only measure the position of an infinitesimal point on the surface. A running average of 80 points of the CS profile, which is equivalent to one voxel, will reduce the *Ra* value by approximately 0.5 µm without applying the λs filter.

As the effect of the instruments' transfer function cannot be modelled using linear regression [55], a power fitting model is preferred to correct the XCT roughness results using the CS roughness traceability route. To this end, any fitting model that assures the *Ra* does not take negative values could also be used. In a specific case, the linear model will predict negative *Ra* values at the lower end, which is impossible because *Ra* is always positive. Figure 12 and Figure 13 presents the calibration curves for the two measurement bandwidths, λs = 80 µm λc = 800 µm and λs = 80 µm λc = 2.5 mm, respectively.

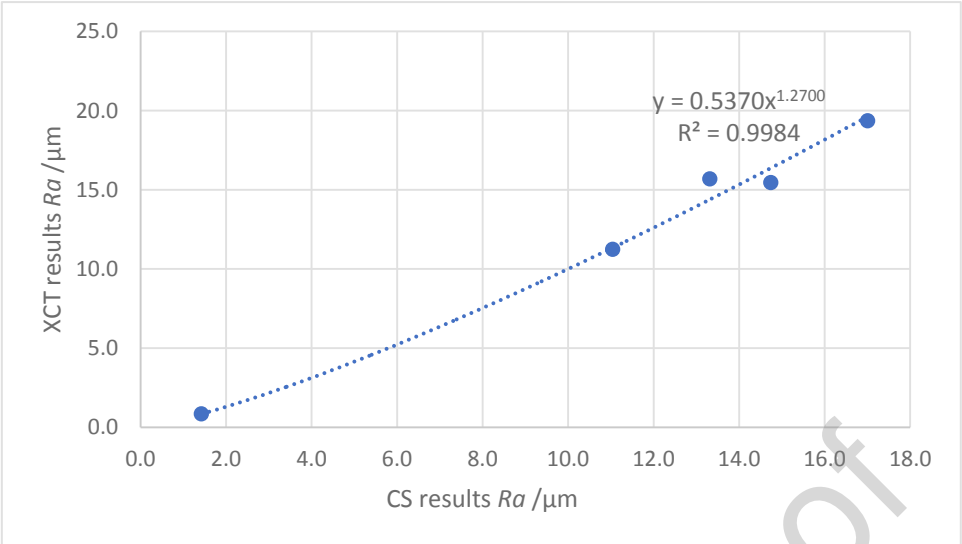

Figure 12 Relationship between XCT and CS data with the filter of λs = 80 µm λc = 800 µm, with no scale correction applied.

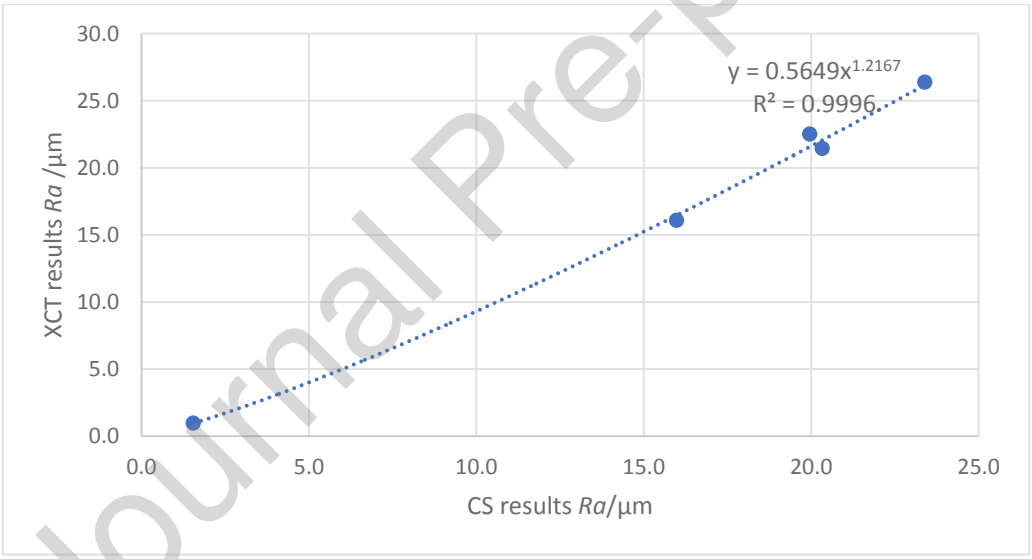

Figure 13 Relationship between XCT and CS data with the filter of λs = 80 µm λc = 2.5 mm, with no scale correction applied.

3.4 Uncertainty framework

The uncertainty evaluation of surface texture using a calibrated reference standard follows the general guideline defined in GUM [51]. In the case of XCT surface roughness measurement traceability established *via* an AM roughness comparison specimen, the main uncertainty contributors can be listed as follows:

- The standard deviation of the mean measurement results and propagated as a normal distribution $N(0,\sigma_{\mathrm{XCT}}^2)$ – Type A standard uncertainty component.

- Roughness specimen calibration which provides the traceability to the unit of length, in this case established *via Ra* evaluation using a traceable CS instrument, propagated as a normal distribution $N(0,u^2_{\mathrm{CS-cal}})$ – Type B standard uncertainty component, where u_{cal} is the combined standard uncertainty calculated as the expanded uncertainty divided by the coverage factor.

  Note that the sphere measurements are not included here as the CS carries the traceability information. The voxel calibration performed with CMS and presented in section 3.1 also confirms that the uncertainty associated with the scale sensitivity factor or "amplification" will not contribute significantly towards the overall uncertainty associated with texture measurements.

  If the standard deviation of the measurement results is available in calibration certificate (σ_{CS} in our case), it can be accounted as a Type A component and propagated as a normal distribution $N(0,\sigma^2_{\mathrm{CS}})$, with the caveat that the combined standard uncertainty associated with roughness specimen calibration can be separated in its constituent Type A and Type B standard uncertainties ($u_{B,CS-cal}$).
- Correction curve errors (δ_{i}) are propagated as one-sided rectangular distributions $R(0,\delta_{\mathrm{i}})$, hence the need for a divisor equal to $3^{-½}$ – Type B standard uncertainty component.

The measurement reproducibility, evaluated as the standard deviation of three repeated measurements, is negligible compared to surface reproducibility (σ_{CS}).

All the uncertainty components listed above are evaluated from the direct measurement of *Ra*, hence their corresponding sensitivity coefficients are equal to 1. In our case, the combined standard measuring uncertainty associated with the corrected *Ra* values ($u_{\mathrm{c\text{-}Ra}}$) can be calculated using the flowing equations:

$$u_{\mathrm{c-Ra}} = \sqrt{u_A^2 + u_{\mathrm{B}}^2}$$

$$u_{\mathrm{A}} = \sqrt{\sigma_{XCT}^2 + \sigma_{CS}^2}$$

$$u_{\mathrm{B}} = \sqrt{\frac{\delta^2}{3} + u^2_{\mathrm{B,CS-cal}}}$$

$$u_{\mathrm{c-Ra}} = \sqrt{\sigma_{XCT}^2 + \sigma_{CS}^2 + \frac{\delta^2}{3} + u^2_{\mathrm{B,CS-cal}}}$$

When the value of σ_{CS} is not explicitly declared in the certificate, the equation above becomes:

$$u_{\mathrm{c-Ra}} = \sqrt{\sigma_{XCT}^2 + \frac{\delta^2}{3} + u_{\mathrm{CS-cal}}^2}$$

The expanded uncertainty is often calculated using a coverage factor $k = 2$, to give a 95 % confidence interval. However, this is correct only when the Type A standard uncertainty is small compared to combined standard uncertainty, which is not the case here. Instead, the Welch Satterthwaite formula should be used to calculate the effective degrees of freedom, which lead to different coverage factors, ranging from 2.37 to 2.11 for a 95 % coverage interval. The value of the combined standard uncertainty is mostly governed by the value of the Type A standard uncertainty, which is mostly affected by the 3DRS surface reproducibility. See Table 3 below.

Table 3 Summary of uncertainty calculations for λc = 2.5 mm case

λc/ mm	Uncertainty component	Face A	Face B	Face C	Face D	SH surface
		/µm				
2.5	u_{A}	1.19	1.25	1.27	0.99	0.06
	u_{B}	0.14	0.44	0.18	0.54	0.05
	u_{C}	1.19	1.32	1.29	1.13	0.08

4 Conclusion

In this paper, we have demonstrated a simple and effective way to provide XCT surface texture measuring traceability for AM surfaces *via* profile method and a unique reference standard with AM roughness and registration features. The work highlights what uncertainties can realistically be achieved in an well controlled shop floor environment when conducting XCT surface texture measurements of AM products. As we have navigated our way through the extant problems encountered with the evaluation and traceability of AM surfaces using XCT, and with the aid of a reference standard developed by NPL, namely 3DRS, we have derived an expanded uncertainty marginally less than 18 % of the measured *Ra* value, most of which is attributed to the surface profile measuring reproducibility. Given the results presented in section 3.3, it can be postulated that the areal method could counteract the profile measurement reproducibility and produce repeatable results with a fraction of the current Type A standard uncertainty. This is not unexpected, as it is well known that the areal method provides superior statistical relevance compared to profile methods; however, the choice of analysis here has been mostly driven by the industrial need for simple traditional roughness measurement traceability. It is also worth pointing out how much the AM surface uniformity affects the profile measurements reproducibility. There is a large gap in the

current additive manufacturing technology's ability to produce AM reference artefacts to the expected level of surface texture uniformity in a cost-effective manner, however, areal characterisation can overcome this issue. The other avenue to further improve uncertainty evaluation is to increase the number of repeat measurements. With the well-established procedure and reference sample, the calibration process can be automated, which reduce burden for operators to implement more measurements and data analyses.

Nevertheless, the work is far from over as there are multiple questions that have yet to be addressed in order to provide adequate trust in the XCT surface texture measurement of AM surfaces. Here we have managed to provide a specific solution to a specific application. However, the functional performance of the AM components may rely on different characteristics of the surface at a different scale. The well-known complexity of AM structures and surfaces poses tremendous challenges for the measurement technology, especially in the absence of clear guidelines that specify the surface texture assessment rules. Besides XCT, current measurement technology is intrinsically 2D and 2½ D in nature and can be easily overwhelmed by the AM surface texture measurement needs, especially in the presence of complex structures and surfaces with overhangs, voids and high slopes. The required confidence in XCT surface texture measurements is yet to be established, given the large number of systematic effects influencing measurements. These pondering issues can lead to an "AM reference standards rush", a familiar and yet to be avoided trend in surface metrology.

Acknowledgement:
This work was supported by EURAMET Joint Research Project 17IND08 AdvanCT which received funding from the EMPIR programme co-financed by the Participating States and from the European Union's Horizon 2020 research and innovation programme. This work was also funded by the UK Government's Department for Business, Energy and Industrial Strategy (BEIS) through the UK's National Measurement System programmes and Centre for Doctoral Training (CDT) in Ultra Precision at Cranfield University which is supported by the RCUK via Grant No.: EP/K503241/1.

References

1 Flys O, Johansson M, Hosseini S B, et al. 2020 Heat transfer and flow performance in additively manufactured cooling channels with varying surface topography *Journal of the Japan Society for Precision Engineering* **86**(1) 71-9 https://doi.org/10.2493/jjspe.86.71.

2 Greitemeier D, Donne C D, Syassen F, et al. 2016 Effect of surface roughness on fatigue performance of additive manufactured Ti–6Al–4V *Mater. Sci. Technol.* **32**(7) 629-34 https://doi.org/10.1179/1743284715Y.0000000053.

3 Brika S E, Letenneur M, Dion C A, et al. 2020 Influence of particle morphology and size distribution on the powder flowability and laser powder bed fusion manufacturability of Ti-6Al-4V alloy *Addit. Manuf.* **31**(100929) 16 https://doi.org/10.1016/j.addma.2019.100929.

4 Haferkamp L, Spierings A, Rusch M, et al. 2021 Effect of particle size of monomodal 316L powder on powder layer density in powder bed fusion *Prog. Addit. Manuf.* **6** 367-74 https://doi.org/10.1007/s40964-020-00152-4.

5 M.A.Balba, A.Ghasemi, E.Fereiduni, et al. 2021 Role of powder particle size on laser powder bed fusion processability of AlSi10mg alloy *Addit. Manuf.* **37**(101630) https://doi.org/10.1016/j.addma.2020.101630.

6 Jacob G, Brown C U, and Donmez A 2018 The influence of spreading metal powders with different particle size distributions on the powder bed density in laser-based powder bed fusion Processes *Advanced Manufacturing Series (NIST AMS), National Institute of Standards and Technology, Gaithersburg, MD, [online]* 26 https://doi.org/10.1016/j.addma.2020.101807.

7 Leicht A, Fischer M, Klement U, et al. 2021 Increasing the productivity of laser powder bed fusion for stainless steel 316L through increased layer thickness *J. Mater. Eng. Perform.* **30** 575-84 https://doi.org/10.1007/s11665-020-05334-3.

8 Kyogoku H and Ikeshoji T-T 2020 A review of metal additive manufacturing technologies: Mechanism of defects formation and simulation of melting and solidification phenomena in laser powder bed fusion process *Mech. Eng. Rev.* **7**(1) 7636-47 https://doi.org/10.1299/mer.19-00182.

9 Yahya Mahmoodkhani, Usman Ali, Shahriar Imani Shahabad, et al. 2019 On the measurement of effective powder layer thickness in laser powder-bed fusion additive manufacturing of metals *Prog. Addit. Manuf.* **4** 109-16 https://doi.org/10.1007/s40964-018-0064-0.

10 Townsend A, Senin N, Blunt L, et al. 2016 Surface texture metrology for metal additive manufacturing: a review *Precis. Eng.* **46** 34-47 https://doi.org/10.1016/j.precisioneng.2016.06.001.

11 Thompson A S N, Giusca C and Leach R 2017 Topography of selectively laser melted surfaces: A comparison of different measurement methods *CIRP Ann. - Manuf. Technol.* **66** 543-6 https://doi.org/10.1016/j.cirp.2017.04.075.

12 Triantaphyllou A, Giusca C L, Macaulay G D, et al. 2015 Surface texture measurement for additive manufacturing *Surf. Topogr.: Metrol. Prop.* **3**(2) 8 https://10.1088/2051-672X/3/2/024002.

13 Turner B N and Gold S A 2015 A review of melt extrusion additive manufacturing processes: II. Materials, dimensional accuracy, and surface roughness *Rapid Protogyp. J.* **21**(3) 250-61 https://doi.org/10.1108/RPJ-02-2013-0017.

14 Snyder J C, Stimpson C K, Thole K A, et al. 2015 Build direction effects on microchannel tolerance and surface roughness *J. Mech. Des.* **137**(111411) 7 https://10.1115/1.4031071.

15 Narasimharaju S R, Liu W, Zeng W, et al. 2021 Surface texture characterization of metal selective laser melted part with varying surface inclinations *J. Tribol.* **143**(5) 1-37 https://doi.org/10.1115/1.4050455.

16 Newton L, Senin N, Chatzivagiannis E, et al. 2020 Feature-based characterisation of Ti6Al4V electron beam powder bed fusion surfaces fabricated at different surface orientations *Addit. Manuf.* **35**(101273) 13 https://10.1016/j.addma.2020.101273.

17 Brown C A, Hansen H N, Jiang X J, et al. 2018 Multiscale analyses and characterizations of surface topographies *CIRP Ann. - Manuf. Technol.* **67**(2) 839-62 https://doi.org/10.1016/j.cirp.2018.06.001.

18 Kozior T, Bochnia J, Zmarzły P, et al. 2020 Waviness of freeform surface characterizations from austenitic stainless steel (316L) manufactured by 3D printing-selective laser melting (SLM) technology *Materials* **13**(19) 4372 https://doi.org/10.3390/ma13194372.

19 Yasa E, Poyraz O, Solakoglu E U, et al. 2016 A study on the stair stepping effect in direct metal laser sintering of a nickel-based superalloy *Procedia CIRP* **45** 175-8 https://doi.org/10.1016/j.procir.2016.02.068.

20 Rott S, Ladewig A, Friedberger K, et al. 2020 Surface roughness in laser powder bed fusion – Interdependency of surface orientation and laser incidence *Addit. Manuf.* **36**(101437) https://doi.org/10.1016/j.addma.2020.101437.

21 Leach R K, Giusca C L, Haitjema H, et al. 2015 Calibration and verification of areal surface texture measuring instruments *CIRP Ann. - Manuf. Technol.* **64**(2) 797-813 https://doi.org/10.1016/j.cirp.2015.05.010.

22 Townsend A, Racasan R, Leach R, et al. 2018 An interlaboratory comparison of X-ray computed tomography measurement for texture and dimensional characterisation of additively manufactured parts *Addit. Manuf.* **23** 422-32 https://doi.org/10.1016/j.addma.2018.08.013.

23 Zanini F, Pagani L, Savio E, et al. 2019 Characterisation of additively manufactured metal surfaces by means of X-ray computed tomography and generalised surface texture parameters *CIRP Ann. - Manuf. Technol.* **68** 515-8 https://doi.org/10.1016/j.cirp.2019.04.074.

24 BS EN ISO 14638 2015 Geometrical product specifications (GPS) — Matrix model BSI Standards Publication

25 Schmitt R and Niggemann C 2010 Uncertainty in measurement for x-ray-computed tomography using calibrated work pieces *Meas. Sci. Technol.* **21**(5) 054008-17

26 Müller P, Hiller J, Dai Y, et al. 2014 Estimation of measurement uncertainties in X-ray computed tomography metrology using the substitution method *CIRP Journal of Manufacturing Science and Technology* **7**(3) 222-32

27 Müller P, Hiller J, Cantatore A, et al. 2012 A study on evaluation strategies in dimensional X-ray computed tomography by estimation of measurement uncertainties *International Journal of Metrology and Quality Engineering* **3**(2) 107 - 15

28 Townsend A, Pagani L, Scott P, et al. 2017 Areal surface texture data extraction from X-ray computed tomography reconstructions of metal additively manufactured parts *Precis. Eng.* **48** 254-64

29 Zanini R, Sbettega E, Sorgato M, et al. 2019 New approach for verifying the accuracy of X-ray computed tomography measurements of surface tpographies in additively manufactured metal parts *J. Nondestr. Eval.* **38**(12) https://doi.org/10.1007/s10921-018-0547-4.

30 PD CEN ISO-TS 15530-1-2013 Geometrical product specifications (GPS) - coordinate measuring machines (CMM): technique for determining the uncertainty of measurement-Part1: overview and metrological characteristics

31 BS EN ISO 3274:1998 1998 Geometric product specifications (GPS). Surface texture. Profile method. Nominal characteristics of contact (stylus) instruments

32 Klingaa C G, Zanini F, Mohanty S, et al. 2021 Characterization of geometry and surface texture of AlSi10Mg laser powder bed fusion channels using X-ray computed tomography *Appl. Sci.* **11**(9) 25

33 Moylan S, Slotwinski J, Cooke A, et al. 2012 Proposal for a standardized test artifact for additive manufacturing machines and processes *Solid Freeform Fabrication Symposium. Proceedings of the Solid Freeform Fabrication Symposium* Austin, TX: NIST p 19

34 Gibson I, Rosen D, and Stucker B 2015 *Additive manufacturing technologies - 3D printing, rapid prototyping, and direct digital manufacturing*. (Springer)

35 Fox J C, Moylan S P, and Lane B M 2016 Effect of process parameters on the surface roughness of overhanging structures in laser powder bed fusion additive manufacturing *Prcedia CIRP* **45** 131-4

36 Tan K L and Yeo S H 2020 Surface finishing on IN625 additively manufactured surfaces by combined ultrasonic cavitation and abrasion *Additive Manufacturing for the Aerospace Industry* **31**

37 Witkin D B, Patel D N, Helvajian H, et al. 2019 Surface treatment of powder-bed fusion additive manufactured metals for improved fatigue life *J. Mater. Eng. Perform.* **28** 681-92

38 Yang L, Gu H, and Lassell A 2014 Surface treatment of Ti6al4V parts made by powder bed fusion additive manufacturing processes using electropolishing *Solid Freeform Fabrication Symposium* Austin, TX p 10

39 Udroiu R, Braga I C, and Nedelcu A 2019 Evaluating the quality surface performance of additive manufacturing systems: methodology and a material jetting case study *materials* **12** 24 https://10.3390/ma12060995.

40 Rubert & Co Ltd Visited on 06/08.2021 *The home of surface measurement* Available from: www.rubert.co.uk/comparison-specimens/

41 DigitalAlloys Visited on 14/03/2021 *Digital alloys' guide to metal additive manufacturing – Part 11 Surface roughness* 2019 Available from: www.digitalalloys.com/blog/surface-roughness/

42 Shah P, Racasan R, and Bills P 2016 Comparison of different additive manufacturing methods using computed tomography *Case Studies in Nondestructive Testing and Evaluation* **6**(Part B) 69-78 https://doi.org/10.1016/j.csndt.2016.05.008.

43 Leach R K 2010 *Fundamental principles of engineering nanometrology*. (Elsevier)

44 Thompson A, Senin N, Maskery I, et al. 2018 Effects of magnification and sampling resolution in X-ray computed tomography for the measurement of additively manufactured metal surfaces *Precis. Eng.* **53** 54-64

45 Leach R, Haitjema H, Su R, et al. 2021 Metrological characteristics for the calibration of surface topography measuring instruments: a review *Meas. Sci. Technol.* **32**(032001) 16 https://10.1088/1361-6501/abb54f.

46 BS EN ISO 25178- 600 2019 Geometrical product specifications (GPS) - Surface texture: Areal part 600: Metrological characteristics for areal topography measuring methods

47 BS EN ISO 15530-3:2011 Geometrical product specifications (GPS) — Coordinate measuring machines (CMM): Technique for determining the uncertainty of measurement Part 3: Use of calibrated workpieces or measurement standards (ISO 15530-3:2011)

48 BS EN ISO 5436-1 2001 Geometrical product specifications (GPS) — Surface texture: Profile method; Measurement standards — Part 1: Material measures

49 BS ISO 4288:1996 1996 Geometric Product Specification (GPS) — Surface texture — Profile method: Rules and procedures for the assessment of surface texture

50 BS EN ISO 4287:2000 2000 Geometrical product specification (GPS) --Surface texture: Profile method -- Terms,definitions and surface texture parameters

51 2008 *Evaluation of measurement data - Guide to the expression of uncertainty in measurement* JCGM 100:2008 GUM 1995 with minor corrections p 120 BPIM

52 Sun W, Brown S, Flay N, et al. 2016 A reference sample for investigating the stability of the imaging system of X-ray computed tomography *Meas. Sci. Technol.* **27**(8)

53 Leach R K 2014 *The measurement of surface texture using stylus instruments* Good Practice Guide No. 37

54 Leach R and Haitjema H 2010 Bandwidth characteristics and comparisons of surface texture measuring instruments *Meas. Sci. Technol.* **21** 9 https://10.1088/0957-0233/21/7/079801.

55 Haijema H and Leach R 2018 *CIRP Encyclopaedia of production engineering, Surface texture metrological characteristics* ed Laperrière L, et al.Berlin, Heidelberg: Springer

CRediT authorship contribution statement

Wenjuan Sun, Writing - Original Draft, Resources, Conceptualization, Methodology, Formal analysis, Funding acquisition, Project administration

Claudiu Giusca, Writing - Review & Editing, Methodology, Funding acquisition

Shan Lou, Writing - Review & Editing

Xiuyuan Yang, Visualization

Xiao Chen, Visualization

Tony Fry, Supervision

Xiangqian Jiang, Supervision

Alan Wilson, Investigation

Stephen Brown, Investigation

Hal Boulter, Investigation

Declaration of interests

☒ The authors declare that they have no known competing financial interests or personal relationships that could have appeared to influence the work reported in this paper.

☐ The authors declare the following financial interests/personal relationships which may be considered as potential competing interests:

2021-12-14

Establishment of X-ray computed tomography traceability for additively manufactured surface texture evaluation

Sun, Wenjuan

Elsevier

Sun W, Giusca C, Lou S, et al., (2022) Establishment of X-ray computed tomography traceability for additively manufactured surface texture evaluation. Additive Manufacturing, Volume 50, February 2022, Article number 102558